Journal of Microbiology, Immunology and Infection 58 (2025) 138–147

Contents lists available at ScienceDirect

Journal of Microbiology, Immunology and Infection

journal homepage: www.e-jmii.com

Interaction of human neutrophils with *Trichomonas vaginalis* protozoan highlights lactoferrin secretion

Wei-Hung Cheng [a,*], Ruei-Min Chen [b], Seow-Chin Ong [b], Yuan-Ming Yeh [c,d,e], Po-Jung Huang [c,f], Chi-Ching Lee [c,g]

[a] *Department of Parasitology, College of Medicine, National Cheng Kung University, Tainan, Taiwan*
[b] *Department of Parasitology, College of Medicine, Chang Gung University, Guishan Dist., Taoyuan City, Taiwan*
[c] *Genomic Medicine Core Laboratory, Chang Gung Memorial Hospital, Linkou, Taiwan*
[d] *Graduate Institute of Health Industry Technology, Chang Gung University of Science and Technology, Taoyuan, Taiwan*
[e] *Graduate Institute of Biomedical Sciences, College of Medicine, Chang Gung University, Taoyuan, Taiwan*
[f] *Department of Biomedical Sciences, College of Medicine, Chang Gung University, Guishan Dist., Taoyuan City, Taiwan*
[g] *Department of Computer Science and Information Engineering, College of Engineering, Chang Gung University, Guishan Dist., Taoyuan City, Taiwan*

ARTICLE INFO

Keywords:
Trichomonas vaginalis
Neutrophils
Excretory-secretory proteins
Cell-to-cell interaction
Proteomics analysis
Lactoferrin

ABSTRACT

Background: Neutrophils are vital constituents of the immune response in the vaginal environment, playing a pivotal role in the defense against trichomoniasis. Earlier studies have shown that *Trichomonas vaginalis* (*T. vaginalis*) can release leukotriene B4 (LTB4), a molecule that attracts and activates neutrophils. Additionally, secretory products from this parasite can induce the production of interleukin-8 (IL-8) in mast cells and neutrophils, which further recruits neutrophils to the infection site. The precise reasons behind *T. vaginalis* actively promoting interaction between parasites and neutrophils rather than inhibiting the inflammatory response remain unclear.

Results: In this study, we collected conditioned medium to elucidate the intricate dynamics between *T. vaginalis* and human neutrophils. We conducted a comprehensive profiling of soluble excretory/secretory proteins (ESPs), identifying 192 protein spots, of which 94 were successfully characterized through mass spectrometry analysis. Notably, the majority of induced ESPs from co-cultivation exhibited consistency with the trichomonad and neutrophil standalone groups, except for lactoferrin, which was observed exclusively following the interaction between neutrophils and *T. vaginalis*. The secretion of lactoferrin was determined to be a contact-dependent process. It was interesting to identify the ability of the iron-loaded lactoferrin to extend the survival time of *T. vaginalis* under iron-deficient conditions.

Conclusions: This study represents the first to identify the origin of lactoferrin during *T. vaginalis* infection, shedding light on the potential reason for *T. vaginalis*'s ability to attract neutrophils to the infection site: the acquisition of the iron source, lactoferrin.

1. Introduction

Trichomoniasis is the most prevalent sexually transmitted infection (STI) of non-viral origin in humans, caused by the parasitic protozoan *Trichomonas vaginalis* (*T. vaginalis*). Clinical reports indicate that more than 200 million new cases are reported annually; this number could exceed the total instances of all STIs caused by bacteria infection.[1–3] *T. vaginalis* resides in the urogenital tract and induces various clinical features in both genders, ranging from asymptomatic carriers to severe inflammation. While trichomoniasis is typically self-limiting in males, it poses serious health problems in female patients, including an increased risk of cervical cancer, pelvic inflammatory disease, infertility, and transmission of HIV.[4,5] The development of trichomoniasis treatment can be traced back to the 1950s; tinidazole and derivatives were the initial choices in clinics. Unfortunately, cumulative reports indicate resistance to these commonly used therapies. Consequently, the pursuit of new therapeutic targets has emerged as the primary goal in the control of trichomoniasis.

A subset of the human population harbors *T. vaginalis* infection without apparent clinical manifestations, suggesting an intricate

* Corresponding author. Department of Parasitology, College of Medicine, National Cheng Kung University No. 1 University Road, Tainan City, 701, Taiwan.
E-mail address: whcheng@gs.ncku.edu.tw (W.-H. Cheng).

https://doi.org/10.1016/j.jmii.2024.11.004
Received 25 July 2024; Received in revised form 14 October 2024; Accepted 12 November 2024
Available online 14 November 2024

balance between the host and the parasite. Moreover, the high recurrence rate observed in trichomoniasis implied, at least in part, an insufficient immune response against *T. vaginalis* invasion. The mucosal layer, comprising epithelial and stromal cells, serves as the primary defense barrier against exogenous pathogens within the vaginal environment. The direct interaction of *T. vaginalis* with vaginal epithelial cells (VECs) constitutes the crucial initial step for successful colonization. *T. vaginalis*–induce alternations in the VECs trigger the secretion of interleukin-8 (IL-8), an inflammatory mediator that recruits innate immune cells to the infection site, including macrophages, mast cells, and neutrophils.[6–8] Neutrophils emerge as the predominant innate immune cell activated by *T. vaginalis* infection.[9–11] Activated neutrophils release granules containing toxic materials, cytokines (IL-8), chemoattractant (leukotriene B4, LTB4), anti-microbial free radicals, and nitric oxide (NO).[7,12] Additionally, neutrophils exhibit trichomonacidal activity through trogocytosis, especially when encountering a limited number of trichomonad cells relative to the neutrophil population.[13] Despite the engagement of both innate and adaptive immune systems against *T. vaginalis*, these responses fall short of eliminating the parasite or preventing the host's susceptibility to secondary infection.

The activation of mast cells, lymphocytes, macrophages, and neutrophils is orchestrated by trichomonad-secreted molecules.[8,14–17] Initial investigations into the excretory/secretory proteins (ESPs) of *T. vaginalis* identified trichomonad adhesion protein 65 (AP-65) as a secreted protein capable of inducing IL-8 production in VECs.[6] Subsequent investigation revealed that TvESP modulates the gene expression of dendritic cells, suggesting a broader impact on immune responses.[16] Additionally, the trichomonad ESP comprises specific proteins that mimic host immune modulators. For instance, *T. vaginalis* secretes a macrophage migration inhibitory factor (MIF)-like protein, influencing inflammation and macrophage functions during infection.[18] The presence of LTB4 homolog derived from *T. vaginalis* has been identified, impacting the activities of neutrophil and mast cells.[19,20] Interestingly, LTB4 attracts neutrophils to the infection site, seemingly presenting a dangerous signal for *T. vaginalis*. Accordingly, the recruitment of neutrophils is triggered by the host epithelial and the *T. vaginalis*. However, the reason behind the protozoan attraction of immune adversaries remains a contentious subject.

It is known that the proliferation and viability of *T. vaginalis* depend on the availability of iron.[21,22] Nonetheless, the iron supply, particularly in the form of free iron, within the vaginal milieu is not consistently abundant. Lactoferrin, renowned for its microbiocidal properties against invading microorganisms, is crucial in iron sequestration.[23,24] The apo-lactoferrin is mainly secreted by the secondary granules of neutrophils, epithelial cells, and exocrine glands, such as the mammary gland.[25–27] The high iron binding affinity makes lactoferrin an efficient carrier and mediates several immunological events.[28–30] Evidence suggests that pathogens, including *Leishmania* spp. and *T. vaginalis*, exploit iron-loaded lactoferrin as a source of iron.[25,27] *T. vaginalis* has specific lactoferrin receptors facilitating iron-dependent enzyme activities.[21] However, the origin of lactoferrin secretion in *T. vaginalis* infection remains unexplored.

This study established a co-culture platform to explore the interaction between human neutrophils and *T. vaginalis* systematically. ESPs were collected from neutrophils, *T. vaginalis*, and their co-cultivations. Notable alterations in ESP composition were documented, with specific emphasis on lactoferrin secretion by neutrophils in response to trichomonad stimulation. A further experiment showed that lactoferrin secretion is a contact-dependent response. Moreover, *T. vaginalis* used iron-loaded lactoferrin to enhance viability under iron-deficient conditions. This report would be the first to investigate the cellular origin of lactoferrin in *T. vaginalis* infection.

2. Materials and methods

2.1. T. vaginalis culture and treatments

T. vaginalis (ATCC30236) was maintained at 37 °C in yeast extract, iron-serum (YI-S) medium containing 10 % horse serum.[31] Mid-log phase cells (~2×10^6/ml) were obtained for experiments. The trypan blue exclusion assay was used to monitor the growth and viability of trichomonad cells. The iron-deficient cells were cultured in YI-S containing 180 μM of dipyridyl (DIP). The iron saturated-lactoferrin (Sigma-Aldrich, L1294) was added to the iron-deficient cultured trichomonad cells in 1 and 2 mg/mL.

2.2. Human neutrophil collection

This study was approved by the Chang Gung Medical Foundation Institutional Review Board (201802178B0) and conducted in accordance with the ethical standards noted in the 1964 Declaration of Helsinki and its later amendments. The blood samples and informed consent were obtained from 25 male and 25 female volunteers from March to July 2018 at Chang Gung University, Taoyuan, Taiwan. Whole blood was collected in a heparin syringe and centrifuge at 650×*g* for 10 min at 25 °C. The plasma was removed, and the precipitated blood cells were transferred to the conical tube containing an equal volume of 3 % Dextran (Amersham Bioscience) and gently mixed. The tube was left static for 25 min at 25 °C. The supernatant from the tube containing 3 % Dextran was slowly added to a new conical tube with the freshly prepared ficoll (Amersham Bioscience). The tubes were then centrifuged at 400×*g* for 40 min at 20 °C. Monocytes were removed, and the neutrophils (the third layer) were collected into a new tube. The neutrophils were resuspended in freshly prepared 0.45 % NaCl. After centrifugation at 400×*g* for 5 min, the pellet was mixed with 3.5 mL ddH_2O to lyse red blood cells (RBCs) for 30 s. Centrifugation at 200×*g* for 5 min was performed, and the cell pellet was resuspended to collect the purified neutrophils. The purified human neutrophils were visualized and validated prior to further experiments (additional file 1). The cells were maintained in RPMI 1640 containing 10 % FBS for further analysis. All samples were applied to experiments individually.

2.3. Co-culture of neutrophil and T. vaginalis

Approximately 1×10^6 trichomonad cells and human neutrophils (multiplicity of infection (MOI) = 1) were collected and washed once with PBS before being added to serum-free RPMI 1640 medium (pH 7.4) (Gibco, ThermoFisher Scientific). Following a 1-h of incubation, the cells and ESPs were harvested for further analyses.

2.4. Excretory/secretory protein collection and concentration

Cells were removed from the 1-h cultured medium by centrifugation at 500×*g* for 10 min. The supernatant (10 mL) was concentrated to the volume of 200 μL by using Amicon ultra-centrifugal filter devices (10 kDa nominal molecular weight limit, NMWL) from EMD Millipore, and the protein level was measured by Bradford assay (Bio-Rad, U.S.).

2.5. Detection of interleukin-8

IL-8 was detected using the DuoDet ELISA kit according to the manufacturer's instructions. The supernatant from neutrophil culture, mixed with Reagent Diluent, was applied to the Capture Antibody-coated wells in triplicate. After a 2-h incubation, the mixture was aspirated, and the wells were washed twice with a Wash Buffer. The Detection Antibody was added to wells and incubated for 2 h at room temperature. Following two washes with Wash Buffer, Streptavidin-HRP was added. Finally, Substrate Solution was added to each well, and the reaction was stopped by adding Stop Solution. The optical density of the

test wells was determined using a microplate reader (SpectraMax M2e, Molecular Devices, USA) set to 450 nm. The concentration was converted using the standard curve.

2.6. Western blot

The harvested ESPs and whole cell lysates derived from trichomonad cells and human neutrophils were analyzed with GAPDH and β-action antibodies (Abcam), respectively, to ensure the purity and avoid contamination of cellular content as previously.[32] Briefly, 20 μg of each sample was separated by 12 % sodium dodecyl sulfate polyacrylamide gel electrophoresis (SDS-PAGE) and transferred to a nitrocellulose membrane. The membrane with proteins was washed with Tris-buffered saline and Tween 20 (TTBS) and blocked with 5 % milk. The primary antibodies were added (1:2000) and incubated overnight at 4 °C. After the washing steps, the membrane was incubated with HRP substrate, and the signals were illustrated using a UVP BioSpectrum 600 imaging system (UVP, CA, USA).

2.7. Cellular protein extraction

Mid-logarithmic phase cells were harvested by centrifugation at 3000 rpm for 15 min and washed with saline three times. A lysis buffer (8 M urea, 4 % CHAPS) containing protease inhibitors (Roche) was added to the cell pellet. The cells were disrupted by sonication through eight cycles in an ice bath. Subsequently, the supernatant (total soluble protein) was harvested by centrifugation at 13,000 rpm for 15 min at 4 °C.

2.8. Two-dimensional gel electrophoresis and silver staining

The 2D-clean-up kit (GE Healthcare) was used to eliminate impurities from the protein extract. The protein concentration was determined using the Bio-Rad Protein Assay Kit. A quantity of 250 μg of protein was diluted to a final volume of 250 μL in rehydration buffer (8 M Urea, 2 % CHAPS), which contained a trace amount of bromophenol blue. Samples were applied to 13 cm IPG gel strips (GE Healthcare) with a pH 4–7 linear separation range.

Rehydration and isoelectric focusing were carried out in an Ettan IPGphor II (GE Healthcare) with the following settings: 30 V for 12 h, 50 V for 0.5 h, 100 V for 0.5 h, 250 V for 0.5 h, 500 V for 0.5 h, 1000 V for 0.5 h, 4000 V for 0.5 h, and gradient to 8000 V for 45,000 Vh. The focused IPG strips were equilibrated for 15 min in the buffer (50 mM Tris–HCl pH 8.8, 6 M urea, 30 % glycerol, 2 % SDS, and a trace of bromophenol blue) containing 1 % (w/v) dithiothreitol, followed by 15 min in a buffer containing 2.5 % (w/v) iodoacetamide.

Equilibrated IPG strips were separated across 15 % SDS-PAGE gels and sealed with a solution of 0.5 % (w/v) agarose containing a trace of bromophenol blue. Gels were run at 35 mA/gel at 4 °C until the tracking dye migrated to the bottom of the gel. The 2-DE gels were stained as previously described.[33] Each experiment was performed three times to ensure the accuracy of the analyses.

2.9. Protein identification by MALDI-TOF-MS

The silver-stained 2-DE gels were scanned and analyzed using the Phoretix™ 2D analysis software. Condensed protein spots were selected and excised from the gels. Gel pieces were transferred to a 0.5 mL tube and destained in a solution containing 30 mM potassium ferricyanide and 100 mM sodium thiosulphate. Subsequently, they were washed and shrunken using 50 mM ammonium bicarbonate and acetonitrile (ACN) before complete dehydration in a vacuum centrifuge. The gel pieces were rehydrated in an approximately 3-fold volume of trypsin solution (20 μg/ml in 25 mM ammonium bicarbonate) (Promega). Digestion occurred at 37 °C for 16 h.

Peptide extraction was performed twice for 15 min by sonication with 2 μL of extraction buffer (100 % ACN with 1 % trifluoroacetic acid). Peptides were eluted and co-crystallized with a saturated solution on a MALDI-TOF sample plate using 0.5 μL of sample and 0.5 μL matrix. The peptides were analyzed using Ultraflex MALDI-TOF Mass Spectrometer (Bruker Daltonic). An automated database search was conducted using the Biotools protein analysis software (Bruker Daltonic). An in-house protein database based on the putative ORFs of EST contigs was explored using the MASCOT database search engine.

The following search parameters were used: trypsin as the enzyme, the peptide tolerance window set to 100 ppm, allowing one missed cleavage, and carbamidomethyl and oxidized methionine set as fixed and variable modifications, respectively. The protein score is represented as -10 Log(P), where P is the probability that the observed match is random. A global MASCOT score greater than 57 and 81 was considered significant in the TvG3 and NCBI nr databases, respectively ($p \leqq 0.05$).

2.10. Detection of secreted lactoferrin using an enzyme-linked immunosorbent assay (Transwell assay)

Lactoferrin concentration was determined by an ELISA-based method following the manufacturer's instructions (Abcam, ab200015). In brief, the conditioned medium and human lactoferrin recombinant protein were mixed with Sample Diluent and added to wells. The Antibody cocktail was then added to sample/standard wells and incubated for 1 h at room temperature with gentle shaking (400 rpm). The testing wells were washed three times with Wash Buffer. Subsequently, the TMB Development Solution was added to testing wells and incubated for 8 min with gentle shaking. The Stop Solution was added to each well and mixed for 1 min. The optical density of testing wells was determined using a microplate reader SpectraMax M2e (Molecular Devices, USA) set to 450 nm. The concentration was calculated using the standard curve.

For the transwell assay, neutrophils were placed in the bottom well, while *T. vaginalis* was placed in the inner well (0.4 μm, HTS Transwell-96, Corning, USA). The ratio of neutrophils to *T. vaginalis* was 1:1 in a serum-free RPMI 1640 medium. The co-cultivation was incubated for 1 h at 37 °C, and the conditioned medium was collected for lactoferrin assay.

2.11. Statistics analysis

The intensity of protein spots was analyzed using Image J software. The student t-test was utilized to quantify experiment results using GraphPad Prism 5. Asterisks represent the significance of each assay as determined by the *P*-value (*, $P < 0.05$; **, $P < 0.01$; ***, $P < 0.001$).

3. Results

3.1. IL-8 production by human neutrophil was induced by T. vaginalis stimulation

T. vaginalis was cultured in the YI-S medium (pH 5.8), while human cell lines were in the RPMI 1640 medium (pH 7.4). There is noise from the additional serum in the culture medium while collecting ESPs. Therefore, a serum-free culture medium was deemed essential for precise ESP analysis. To test the viability of trichomonad cells without serum supplementation, we harvested the stationary phase trichomonad cells and resuspended them in the RPMI 1640 serum-free medium. The result showed that the number of viable cells ($\sim 10^6$ cells/ml) remained consistent for at least 3 h, indicating *T. vaginalis*'s resilience in RPMI 1640 serum-free medium (Additional file 2a and b).

IL-8 secretion level was used as the indicator to evaluate the ratio of neutrophils and *T. vaginalis* in the co-cultivation system.[6,7,34] Various ratios (20:1, 10:1, 5:1, and 1:1) of neutrophil to *T. vaginalis* were employed, and ELISA detected IL-8 levels in each group. As shown in Additional file 2c, only the 1:1 ratio revealed a significant increase in

IL-8 concentration after 1 h of co-incubation. This established condition served as the standard procedure for all experiments in this study.

3.2. Assessment of trichomonad ESPs

ESPs derived from *T. vaginalis* and human neutrophils were collected and concentrated prior to analyzed by SDS-PAGE (Additional file 3). ESPs are susceptible to contamination with intracellular components during preparation. To ensure that the ESPs were secreted out but not a result of cell destruction, we performed immune blotting to detect intracellular protein markers (GAPDH and β-actin) in the ESPs. As depicted in Fig. 1a and b, the ESPs obtained from T. vaginalis or neutrophils were confirmed to be solely of secreted origin, devoid of cellular proteins because none of these intracellular proteins could be detected in ESP fractions.

Previous reports indicated that T. vaginalis-derived ESPs possess the capability to induce IL-8 secretion in host VECs.[6] To confirm the accurate collection of ESP samples, concentrated ESPs were introduced to human neutrophils in RPMI 1640 serum-free medium, and the secretion of IL-8 was monitored by ELISA. The results demonstrated a time-dependent increase in IL-8 production by neutrophils following the addition of trichomonad-derived ESPs (50 and 100 μg) (Fig. 1c).

3.3. Exhibition of significant changed ESPs after co-cultivation by 2D gel electrophoresis

To elucidate the interaction of *T. vaginalis* with host neutrophils, we subjected ESPs to two-dimensional gel electrophoresis to visualize the alternations following co-incubation of T. vaginalis and neutrophil. In isolation, ESP profiles of T. vaginalis and neutrophils served as the reference gels for subsequent protein comparisons after co-culture. Ninety and 62 protein spots were observed in the conditioned medium of T. vaginalis and neutrophils, respectively (Fig. 2a and b). ESPs derived from a co-cultured medium exhibited 40 protein spots (Fig. 3). By aligning with the reference gels (a) and (b), red and blue circles denoted proteins secreted by T. vaginalis and neutrophil, respectively. In contrast, the remaining protein spots were induced after the cellular communication between the two entities.

3.4. Identification of lactoferrin within the significantly changed ESPs

We extracted proteins from the 2D gels and performed Matrix-Assisted Laser Desorption Ionization Time of Flight (MALDI TOF) analysis to identify proteins secreted following co-cultivation. Ninety trichomonad EPS spots were analyzed, identifying 43 high-confidence proteins numbered in Fig. 2a and listed in Table 1. The presence of glycolytic enzymes, AP65, thioredoxin reductase, and coronin, were previously recognized after VEC co-cultivation,[6] corroborating the informativeness and reliability of our results. Table 2 revealed 51 proteins identified from 62 neutrophil protein spots, with the majority being albumin, excepted, given its abundance in serum.

Table 3 documented proteins secreted after 1 h of trichomonad cell and neutrophil co-culture. Protein spots originating from both cells, such as human albumin and trichomonad triosephosphate isomerase, were highlighted on the gel (Fig. 3, red and blue circles indicated trichomonad- and neutrophil-derived ESPs, respectively). The intensity of protein spots derived from the co-culture group was compared to *T. vaginalis* and human neutrophil controls. The results indicated most of them were reduced after co-culture, except trichomonad lactate dehydrogenase (spot 4) and a human unnamed protein (spot 26) (Additional file 4). Additionally, the newly presented protein spots were identified using trichomonad and human protein databases. Nineteen protein spots, 1, 2, 17, 18, 19, 21, 24, 27, and 30–40, were secreted after co-culture, assuming their roles in stimulation or host-parasite communication. Notably, trichomonad malic enzyme, the sequence ortholog of AP65 (spot 17), was secreted after co-culture, speculating to function as a homolog promoting cytoadherence and enhancing colonization.[35] Alcohol dehydrogenase (spot 18), triosephosphate isomerase (spot 21), heat shock protein 70 (spot 27), ornithine carbamoyltransferase (spot 30), and actin (spot 34) were additional trichomonad responders to the interaction.

Neutrophil-derived proteins, such as annexin V and albumin, were almost comparable before the host-protozoan interaction. The most noticeable protein induced by T. vaginalis was lactoferrin (gi|28948741), a defensive protein that sequesters pathogens by competitively acquiring free iron.[27] However, T. vaginalis possesses lactoferrin receptors that engulf lactoferrin, further enhancing the activity of iron-containing hydrogenosomal enzyme pyruvate: ferredoxin oxidoreductase (PFOR).[36] Interestingly, another iron-carrier protein, transferrin (spots 1 and 2), was secreted by neutrophil before the communication but was not observed after trichomonad stimulation. We speculated this absence may be due to reduced secretion since T. vaginalis does not utilize transferrin as the iron source.[36]

This study provided the first direct evidence that host neutrophils secreted lactoferrin after interacting with T. vaginalis. The mechanism by which lactoferrin mediates interactions between *T. vaginalis* and host

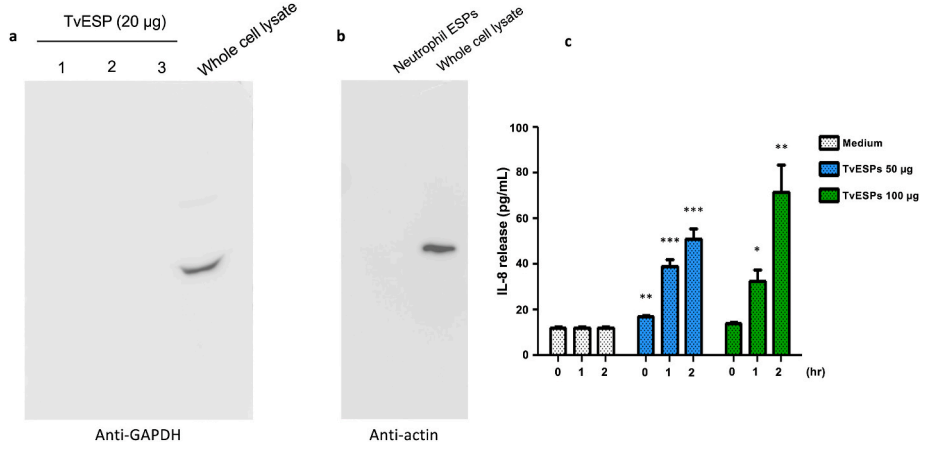

Fig. 1. Trichomonad-derived ESPs trigger IL-8 production in neutrophils. (a, b) The confirmation of ESPs secreted by *T. vaginalis* and neutrophil. Comparing the ESPs to whole cell lysates of the trichomonad cells and neutrophil by immunoblotting using anti-GAPDH and anti-actin antibodies, respectively. (c) The ESPs were collected from RPMI 1640 serum-free medium incubated *T. vaginalis* for 1 h. After ESPs concentration by spin column, 50 and 100×*g* of ESPs were added to the neutrophil, and the IL-8 level was measured every hour. The student t-tests were conducted to compare the trichomonad ESPs treated cells to that of medium control. Significance is indicated by asterisks: $*P < 0.05$; $**P < 0.01$; $***P < 0.001$.

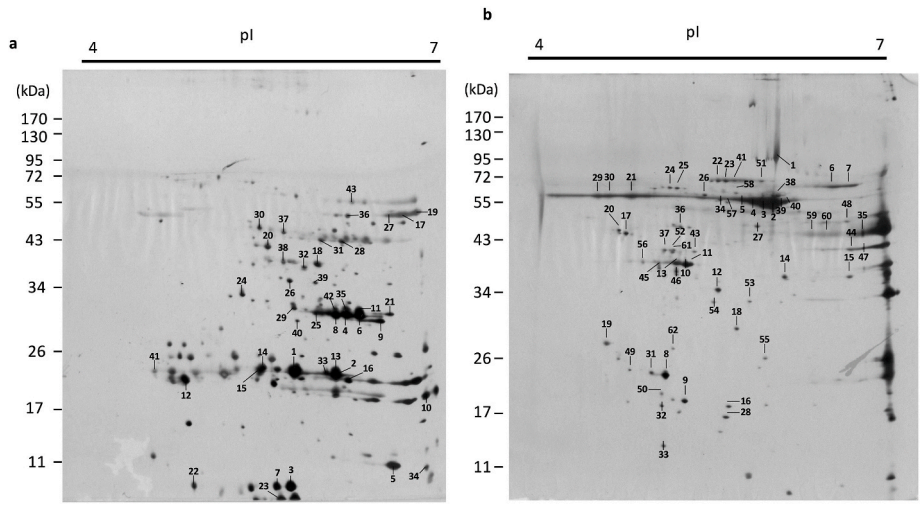

Fig. 2. 2D gel electrophoresis of ESPs derived from *T. vaginalis* and human neutrophils. ESP profiles of *T. vaginalis* (a) and neutrophils (b) were exhibited. Total 90 and 62 protein spots were shown in *T. vaginalis* and neutrophils, respectively.

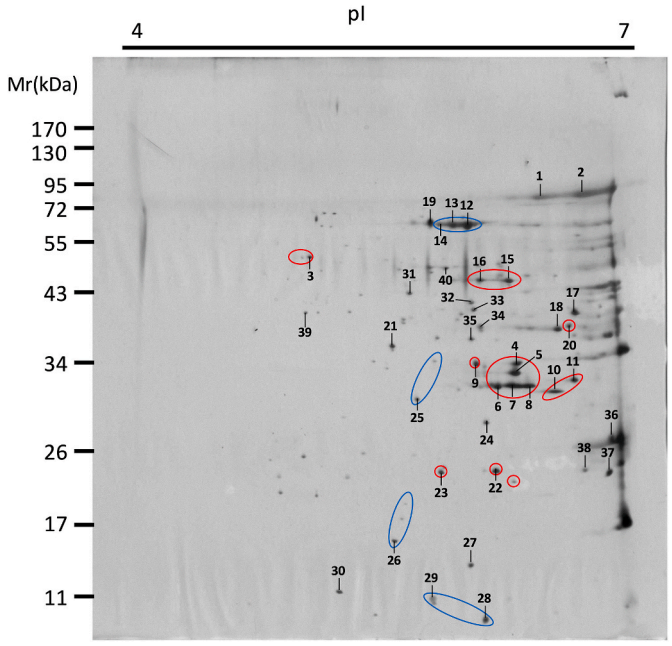

Fig. 3. 2D gel electrophoresis of ESPs after co-culture of T. vaginalis and human neutrophils. ESP profile of co-cultured conditioned medium was exhibited. A total of 40 protein spots were shown. Red and blue circles indicated the presence of ESPs secreted by *T. vaginalis* (10 protein spots) and neutrophil (8 protein spots), respectively, before co-cultivation. Sixteen proteins were shown solely in the co-culture condition.

neutrophils remains unknown and warrants further investigation.

3.5. Lactoferrin is secreted via a contact-dependent interaction

To better understand the actual change in the secretion of lactoferrin by human neutrophils, we quantified the lactoferrin in the conditioned medium upon stimulation by *T. vaginalis* using an ELISA-based method. The results showed a lactoferrin concentration of 600 ng/ml in the stimulated group compared to the control where the lactoferrin concentration was less than 200 ng/ml (Fig. 4). This finding suggested a 3-times augmentation in lactoferrin secretion following exposure to trichomonad cells.

To investigate whether direct cell-to-cell contact with *T. vaginalis* was necessary to provoke lactoferrin secretion by host neutrophils, a transwell assay was employed. Neutrophils were seeded in the bottom well, separated from trichomonad cells in the inner well by a 0.4 μm membrane. As anticipated, no detectable lactoferrin was observed in the inner well (Fig. 4). After the co-incubation in the transwell device, the concentration of lactoferrin in the bottom well was comparable to that of the untreated control (neutrophil only). This result indicated that the secretion of lactoferrin by the host neutrophile is a contact-dependent stimulus in the infection of *T. vaginalis*.

3.6. Holo-Lactoferrin extends the survival time of trichomonad cells upon iron deficiency

Lactoferrin is secreted as an iron-binding protein that sequesters free iron to limit its usage by pathogens.[25] Previous studies showed that trichomonad cells possess lactoferrin receptors to capture the iron-loaded lactoferrin and thus maintain the activity of hydrogenosomal enzymes under iron-limited conditions.[21] As the iron source, the fluctuating lactoferrin content in the vagina could be up to 50-fold between menstrual cycles; therefore, the secretion from neutrophils would be an important source of iron for the protozoan during premenstrual period.[27] By using the iron-limited circumstance, the usage of iron-loaded lactoferrin on the protozoan would be easily observed.[21]

To assess the functionality of lactoferrin serves as the iron source, we treated trichomonad cells with or without holo-lactoferrin under iron-deficient conditions and monitored the viability. As shown in Fig. 5, there was a dose-dependent extension of survival time, lasting at least 48 h, after adding iron-loaded holo-lactoferrin, compared to the untreated group, which dropped cell density after 33 h. Although the survival time extended by holo-lactoferrin, the supplementation of free iron would directly increase the cell density (Additional file 5). This data implied that lactoferrin, when secreted by neutrophil in response to stimulation by T. vaginalis, could confer benefits as the iron carrier for the parasite.

4. Discussion

T. vaginalis infection causes a diverse range of manifestations in both genders, with a significant proportion of patients remaining asymptomatic, posing challenges in disease prevalence control. The attachment of the parasite to vaginal epithelial cells initiates colonization as well as host immune responses.[6,37] Neutrophil is the most abundant immune cell in the vagina, which are likely pivotal in restraining *T. vaginalis*. Despite the host's immune system response, the protozoan

Table 1
The identified ESPs derived from *T. vaginalis*.

Spot	Accession no.	Protein name	Score	Coverage (%)	MW	pI	#P
1	TVAG_096350	Triosephosphate isomerase	85	70 %	27,683	5.76	28
2	TVAG_096350	Triosephosphate isomerase	90	70 %	27,683	5.76	35
3	TVAG_360700	Fructose-1,6-bisphosphate aldolase	67	68 %	36,414	5.88	28
4	TVAG_363390	Fructose-1,6-bisphosphate aldolase	150	93 %	36,467	5.84	46
5	TVAG_360700	Fructose-1,6-bisphosphate aldolase	72	59 %	36,414	5.88	39
6	TVAG_360700	Fructose-1,6-bisphosphate aldolase	168	94 %	36,414	5.88	50
7	TVAG_363390	Fructose-1,6-bisphosphate aldolase	63	49 %	36,467	5.84	29
8	TVAG_043060	Fructose-1,6-bisphosphate aldolase	111	83 %	36,443	5.79	39
9	TVAG_300000	Fructose-1,6-bisphosphate aldolase	139	96 %	36,452	6.02	47
10	TVAG_068130	Malate dehydrogenase:SUBUNIT = A	74	73 %	29,808	8.46	26
11	TVAG_360700	Fructose-1,6-bisphosphate aldolase	100	77 %	36,414	5.88	34
12	TVAG_261970	Carbamate kinase	75	67 %	40,476	5.48	33
13	TVAG_096350	Triosephosphate isomerase	61	59 %	27,683	5.76	21
14	TVAG_096350	Triosephosphate isomerase	68	59 %	27,683	5.76	22
15	TVAG_096350	Triosephosphate isomerase	80	59 %	27,683	5.76	27
16	TVAG_454490	Purine nucleoside phosphorylase	91	57 %	25,854	5.97	20
17	TVAG_340290	Adhesin AP65-1 precursor	101	63 %	63,686	7.22	42
18	TVAG_124870	Coronin	85	67 %	48,424	6.06	38
19	TVAG_340290	Adhesin AP65-1 precursor	90	52 %	63,686	7.22	39
20	TVAG_126970	GDP dissociation inhibitor family protein	82	63 %	49,645	5.57	42
21	TVAG_345360	Fructose-1,6-bisphosphate aldolase	169	89 %	36,543	6.06	48
22	TVAG_192620	Cofilin/tropomyosin-type actin-binding protein	63	72 %	16,078	5.17	19
23	TVAG_038440	Fructose-1,6-bisphosphate aldolase	64	53 %	36,581	5.88	21
24	TVAG_419590	Ornithine cyclodeaminase/mu-crystallin family protein	120	76 %	36,473	5.34	43
25	TVAG_363390	Fructose-1,6-bisphosphate aldolase	98	53 %	36,467	5.84	30
26	TVAG_538040	Ketopantoate reductase pane/apba family protein	88	70 %	37,783	5.69	32
27	TVAG_267870	Malate dehydrogenase:SUBUNIT = A	85	60 %	63,705	8.33	39
28	TVAG_464170	Enolase 4	113	72 %	53,627	6.33	54
29	TVAG_267310	Hypothetical protein	61	34 %	28,950	5.1	13
30	TVAG_405240	Adenosylhomocysteinase	79	60 %	53,873	5.53	39
31	TVAG_464170	Enolase 4	99	66 %	53,627	6.33	41
32	TVAG_392410	Clan MH, family M18, aspartyl aminopeptidase-like metallopeptidase	75	81 %	45,484	5.74	36
33	TVAG_096350	Triosephosphate isomerase	68	59 %	27,683	5.76	28
34	TVAG_300000	Fructose-1,6-bisphosphate aldolase	69	51 %	36,452	6.02	29
35	TVAG_363390	Fructose-1,6-bisphosphate aldolase	76	52 %	36,467	5.84	31
36	TVAG_061930	Glucose-6-phosphate isomerase family protein	118	75 %	61,459	5.94	63
37	TVAG_210320	Adenosylhomocysteinase	93	64 %	54,064	5.61	45
38	TVAG_026290	Hypothetical protein	101	71 %	44,028	5.67	44
39	TVAG_041310	Ornithine carbamoyltransferase family protein	60	71 %	35,578	5.75	29
40	TVAG_202440	Aldose 1-epimerase family protein	70	62 %	34,454	5.82	25
41	TVAG_344070	Hypothetical protein	63	65 %	32,858	6.24	20
42	TVAG_363390	Fructose-1,6-bisphosphate aldolase	99	58 %	36,467	5.84	31
43	TVAG_139300	Phosphoenol pyruvate carboxykinase	63	44 %	67,886	6.07	41

MW, molecular weight; pI, isoelectric point; #P, number of peptides matched.

adeptly evades immune surveillance, leading to persistent infection. Trichomonad ESPs and exosomes have demonstrated alternations in several aspects of the host immune system.[16,17,38] For instance, Tv-ELVs trigger the expression changes in cytokine profiles, including IL-6, IL-8, and IL-10 [38]. However, comprehensive information on the regulations governing host immune cells during *T. vaginalis* infection is lacking, with limited studies focusing on the responses of the parasite to host immune cells. Thus, exploring how *T. vaginalis* interacts with neutrophils becomes an essential issue in understanding the mechanisms underpinning persistent parasitism in the human vagina. This study aimed to elucidate the consequences of the interaction between *T. vaginalis* and neutrophils by identifying ESPs derived after *in vitro* co-cultivation. Leveraging ESP profiles, we highlighted and demonstrated the extracellular effector molecules of *T. vaginalis* in response to neutrophils and vice versa.

Effector proteins, such as cytokines, antibodies, and complement, constitute critical components of the immune system in the surveillance of invading microorganisms in the vaginal region. Despite the pivotal role of humoral immune responses, their efficacy against *T. vaginalis*, even in recurrent trichomoniasis, has been limited. The mechanisms underlying the ineffectiveness of humoral immune responses against *T. vaginalis* have been partially answered. Secretory cysteine proteases (TvCPs) have emerged as the crucial molecule linked to the virulence of *T. vaginalis*. Notably, TvCPs are implicated in hemolysis, cytoadherence, host cell apoptosis, and degradation of antibodies.[37,39–41] Moreover, *T. vaginalis* exhibits resistance to complement because of TvCPs-mediated destruction of the C3 molecule, particularly under iron-sufficient conditions.[37,42] These findings suggest that *T. vaginalis* has evolved multiple mechanisms to modulate human immune responses, thereby facilitating continuous parasitization in the host.

Human parasites have evolved mechanisms to modulate host immune responses, suggesting that parasites might actively initiate the interaction with the host immune system. A multicellular parasite *Fasciola hepatica* produces and secretes a molecule with transforming growth factor (TGF)-like properties, referred to as FhTLM, which has the capacity to modify host immunity. FhTLM binds to TGF-β Receptor II, leading to a reduction in the production of IL-12 and NO by fibroblasts and macrophages. These alternations restrict the immune responses triggered by *F. hepatica*, promoting the establishment of a successful chronic infection.[43] This emphasized the pivotal role of secreted parasite products in modulating host immune responses.

ESPs of *T. vaginalis* are essential mediators for inducing host VEC responses.[6] In a study by Kucknoor et al., 19 trichomonad secretory proteins are identified, with a predominant presence of metabolic enzymes and TvCPs. Serine proteases of *Schistosoma mansoni* play essential roles in the pathogenesis, which induces host fibrinolysis and vasodilatation in order to survive.[44] Therefore, proteolytic enzymes frequently emerge as communicators in the interaction between parasites and their hosts.

Table 2
The identified ESPs derived from neutrophils.

Spot	Accession no.	Protein name	Score	Coverage (%)	MW	pI	#P
1	gi|55669910	Chain A, Crystal Structure Of The Ga Module Complexed With Human Serum Albumin	413	73 %	67174	5.57	47
2	gi|157830361	Chain A, Human Serum Albumin In A Complex With Myristic Acid And Tri- Iodobenzoic Acid	472	85 %	67988	5.69	57
3	gi|55669910	Chain A, Crystal Structure Of The Ga Module Complexed With Human Serum Albumin	417	78 %	67174	5.57	49
4	gi|55669910	Chain A, Crystal Structure Of The Ga Module Complexed With Human Serum Albumin	342	72 %	67174	5.57	44
5	gi|157830361	Chain A, Human Serum Albumin In A Complex With Myristic Acid And Tri- Iodobenzoic Acid	321	65 %	67988	5.69	39
6	gi|62897069	transferrin variant [*Homo sapiens*]	260	38 %	79310	6.68	31
7	gi|115394517	transferrin [*Homo sapiens*]	389	57 %	79190	6.97	46
8	gi|9955206	Chain B, Crystal Structure Of A Rac-Rhogdi Complex	125	62 %	20521	6.16	14
9	gi|90108664	Chain A, Crystal Structure Of Lipid-Free Human Apolipoprotein A-I	236	69 %	28061	5.27	25
10	gi|194388064	unnamed protein product [*Homo sapiens*]	247	65 %	40116	5.23	32
11	gi|16924319	Unknown (protein for IMAGE:3538275), partial [*Homo sapiens*]	176	49 %	40819	5.78	21
12	gi|16924319	Unknown (protein for IMAGE:3538275), partial [*Homo sapiens*]	192	50 %	40819	5.78	21
13	gi|14250401	actin, beta, partial [*Homo sapiens*]	222	58 %	41321	5.56	24
14	gi|442570728	Chain A, Crystal Structure Of Human Serpinb1 Mutant	134	41 %	43969	6.03	14
15	gi|166007012	Chain A, Crystal Structure Of The Human Hsp70 Atpase Domain In The Apo Form	161	56 %	43182	6.35	22
16	gi|20664358	Chain A, Crystal Structure Of A Recombinant Glutathione Transferase, Created By Replacing The Last Seven Residues Of Each Subunit Of The Human Class Pi Isoenzyme With The Additional C-Terminal Helix Of Human Class Alpha Isoenzyme	133	60 %	23430	5.09	13
17	gi|157830132	Chain A, The High Resolution Structure Of Annexin Iii Shows Differences With Annexin V	205	56 %	36480	5.63	23
18	gi|169791854	Chain D, Structure Of The Rap-Rapgap Complex	132	70 %	19161	4.77	13
19	gi|194388374	unnamed protein product [*Homo sapiens*]	88	23 %	1E+05	5.35	21
20	gi|69990	alpha-1-B-glycoprotein - human	233	47 %	52479	5.65	23
21	gi|69990	alpha-1-B-glycoprotein - human	194	47 %	52479	5.65	23
22	gi|225698069	Chain A, Crystal Structure Of Hsc70BAG1 IN COMPLEX WITH ATP	101	46 %	42120	6.38	18
23	gi|220,702,506	Chain A, TapasinERP57 HETERODIMER	122	34 %	54541	5.61	19
24	gi|194375974	unnamed protein product [*Homo sapiens*]	154	67 %	20209	8.9	14
25	gi|157830361	Chain A, Human Serum Albumin In A Complex With Myristic Acid And Tri- Iodobenzoic Acid	249	58 %	67988	5.69	30
26	gi|119626071	albumin, isoform CRA_h [*Homo sapiens*]	185	47 %	70564	5.92	24
27	gi|4757768	rho GDP-dissociation inhibitor 1 isoform a [*Homo sapiens*]	96	39 %	23250	5.02	12
28	gi|90108664	Chain A, Crystal Structure Of Lipid-Free Human Apolipoprotein A-I	147	67 %	28061	5.27	15
29	gi|169791854	Chain D, Structure Of The Rap-Rapgap Complex	138	70 %	19161	4.77	13
30	gi|166007012	Chain A, Crystal Structure Of The Human Hsp70 Atpase Domain In The Apo Form	133	48 %	43182	6.35	15
31	gi|18655424	Chain A, Crystallographic Analysis Of The Human Vitamin D Binding Protein	136	43 %	52780	5.17	16
32	gi|17028367	Similar to gelsolin (amyloidosis, Finnish type), partial [*Homo sapiens*]	77	33 %	31052	4.85	7
33	gi|157830361	Chain A, Human Serum Albumin In A Complex With Myristic Acid And Tri- Iodobenzoic Acid	330	63 %	67988	5.69	40
34	gi|157830361	Chain A, Human Serum Albumin In A Complex With Myristic Acid And Tri- Iodobenzoic Acid	310	69 %	67988	5.69	40
35	gi|157830361	Chain A, Human Serum Albumin In A Complex With Myristic Acid And Tri- Iodobenzoic Acid	341	69 %	67988	5.69	42
36	gi|320089786	Chain A, Crystal Structure Of Human Grp78 (70kda Heat Shock Protein 5 BIP) Atpase Domain In Complex With Atp	146	47 %	42275	6	17
37	gi|203282367	Chain A, Crystal Structure Of Human Enolase 1	141	45 %	47350	6.99	19
38	gi|3337390	haptoglobin [*Homo sapiens*]	83	31 %	38722	6.14	11
39	gi|47124562	HP protein [*Homo sapiens*]	71	36 %	31647	8.48	11
40	gi|203282367	Chain A, Crystal Structure Of Human Enolase 1	141	51 %	47350	6.99	19
41	gi|5902134	coronin-1A [*Homo sapiens*]	73	18 %	51678	6.25	11
42	gi|178045	gamma-actin, partial [*Homo sapiens*]	98	35 %	26147	5.65	10
43	gi|221045102	unnamed protein product [*Homo sapiens*]	112	28 %	79068	5.77	16
44	gi|17028367	Similar to gelsolin (amyloidosis, Finnish type), partial [*Homo sapiens*]	76	40 %	31052	4.85	8
45	gi|48257056	TALDO1 protein, partial [*Homo sapiens*]	103	36 %	37556	6.35	16
46	gi|5453597	F-actin-capping protein subunit alpha-1 [*Homo sapiens*]	139	67 %	33073	5.45	16
47	gi|3337390	haptoglobin [*Homo sapiens*]	70	24 %	38722	6.14	10

(*continued on next page*)

Table 2 (*continued*)

Spot	Accession no.	Protein name	Score	Coverage (%)	MW	pI	#P
48	gi|225698069	Chain A, Crystal Structure Of Hsc70BAG1 IN COMPLEX WITH ATP	97	42 %	42120	6.38	14
49	gi|1335098	unnamed protein product [*Homo sapiens*]	114	30 %	49948	6.43	14
50	gi|17028367	Similar to gelsolin (amyloidosis, Finnish type), partial [*Homo sapiens*]	72	32 %	31052	4.85	7
51	gi|344189840	Chain A, Crystal Structure Analysis Of H74a Mutant Of Human Clic1	151	56 %	26594	5.16	14

MW, molecular weight; pI, isoelectric point; #P, number of peptides matched.

Table 3
The identified ESPs derived from *T. vaginalis* and neutrophils after co-culture.

Spot	Accession no.	Protein name	Score	Coverage (%)	MW	pI	#P[a]
1*	gi|28948741	Chain A, Crystal Structure Of Human Seminal Lactoferrin At 3.4 A Resolution	397	62 %	77928	8.47	43
2*	gi|28948741	Chain A, Crystal Structure Of Human Seminal Lactoferrin At 3.4 A Resolution	481	63 %	77928	8.47	51
3	TVAG_224980	Clan MH, family M20, peptidase T-like metallopeptidase	104	34 %	51857	5.03	11
4	TVAG_381310	lactate dehydrogenase family protein	90	35 %	37243	5.78	12
5	TVAG_253650	malate dehydrogenase	140	54 %	36098	6.4	19
6	TVAG_363390	fructose-1,6-bisphosphate aldolase	273	60 %	36467	5.84	30
7	TVAG_043060	fructose-1,6-bisphosphate aldolase	282	83 %	36443	5.79	30
8	TVAG_360700	fructose-1,6-bisphosphate aldolase	278	63 %	36414	5.88	31
9	TVAG_381310	lactate dehydrogenase family protein	79	32 %	37243	5.78	10
10	TVAG_300000	fructose-1,6-bisphosphate aldolase	268	59 %	36452	6.02	24
11	TVAG_345360	fructose-1,6-bisphosphate aldolase	216	50 %	36543	6.06	25
12	gi|55669910	Chain A, Crystal Structure Of The Ga Module Complexed With Human Serum Albumin	489	79 %	67174	5.57	52
13	gi|157830361	Chain A, Human Serum Albumin In A Complex With Myristic Acid And Tri- Iodobenzoic Acid	388	68 %	67988	5.69	44
14	gi|157830361	Chain A, Human Serum Albumin In A Complex With Myristic Acid And Tri- Iodobenzoic Acid	290	61 %	67988	5.69	31
15	TVAG_464170	enolase 4	310	67 %	53627	6.33	39
16	TVAG_043500	enolase 3	133	32 %	51708	5.89	17
17*	TVAG_491670	malic enzyme; adhesin protein 65 (AP65)	104	36 %	42785	6.39	13
18*	TVAG_228780	alcohol dehydrogenase 1	81	35 %	39471	6.14	10
19*	gi|166007012	Chain A, Crystal Structure Of The Human Hsp70 Atpase Domain In The Apo Form	198	70 %	43182	6.35	23
20	gi|194375299	unnamed protein product [*Homo sapiens*]	119	34 %	37667	5.49	12
21*	TVAG_096350	triosephosphate isomerase	68	33 %	27683	5.76	6
22	TVAG_096350	triosephosphate isomerase	74	25 %	27683	5.76	7
23	TVAG_474980	thioredoxin reductase	115	37 %	32805	6.02	11
24*	gi|157830132	Chain A, The High Resolution Structure Of Annexin Iii Shows Differences With Annexin V	143	32 %	36480	5.63	13
25	gi|194375974	unnamed protein product [*Homo sapiens*]	96	43 %	20209	8.9	7
26	gi|194375974	unnamed protein product [*Homo sapiens*]	79	36 %	20209	8.9	6
27*	TVAG_092490	endoplasmic reticulum heat shock protein 70	141	23 %	71618	5.06	16
28	TVAG_124870	coronin	115	33 %	48424	6.06	13
29	gi|442570728	Chain A, Crystal Structure Of Human Serpinb1 Mutant	106	31 %	43969	6.03	11
30*	TVAG_041310	ornithine carbamoyltransferase family protein	70	30 %	35578	5.75	8
31*	gi|158428858	Chain A, X Ray Structure Of The Complex Between Carbonic Anhydrase I And The Phosphonate Antiviral Drug Foscarnet	81	37 %	28408	6.9	8
32*	TVAG_196620	hypothetical protein	73	43 %	24070	6.32	7
33*	gi|999892	Chain A, Crystal Structure Of Recombinant Human Triosephosphate Isomerase At 2.8 Å Resolution. Triosephosphate Isomerase Related Human Genetic Disorders And Comparison With The Trypanosomal Enzyme	90	36 %	26807	6.51	7
34*	TVAG_200190	actin	76	20 %	42154	5.05	8

MW, molecular weight; pI, isoelectric point; #P, number of peptides matched; *, the newly secreted ESPs identified after co-cultivation.

Most studies have focused on the responses of host immune cells during infection with parasites or protozoa; however, it is crucial to know how parasites respond to host factors. Investigations on helminths had pinpointed the effects upon sensing specific host molecules. For example, in *S. mansoni*, the laying of eggs is stimulated by host tumor necrosis factor-α (TNF-α).[45] Moreover, the maturation of filaria and the birth of microfilaria in human hosts are accelerated in the presence of high levels of IL-5 and eosinophils. Interestingly, IL-5 is the cytoattractant that recruits eosinophils, indicating that host immunity may not restrict but promote filarial parasites' infectivity.[46] Collectively, parasites leverage host molecules, especially immune effectors, to facilitate proper growth or proliferation. This bi-directional interaction may serve as a significant driving force for the evolution of parasites to peacefully survive in the host.

As the predominant innate immune cell population in the vagina, neutrophils are recruited from the bloodstream to the infection site by IL-8 and LTB4, which are secreted by VECs and neutrophils, respectively. The killing modes of trichomonad cells by neutrophils rely on trogocytosis and the secretion of toxic granules.[7,13] In the context of *T. vaginalis* infection, the protozoan secretes LTB4, effectively attracting neutrophils.[9] This phenomenon is intriguing to know the reason for recruiting the host immune cells to a nearby position. We performed a 2DE-based proteomics analysis and showed that lactoferrin was only present after co-cultivation of *T. vaginalis* and human neutrophils. Moreover, by conducting a Transwell assay, it was proven that lactoferrin secretion was a contact-dependent process. Based on our findings, we speculated that the recruitment of human neutrophils to the trichomonad infection site was to initiate a contact-dependent interaction that eventually stimulates the secretion of lactoferrin.

In our 2-DE-based EPS analysis, only a limited number of protein spots emerged after co-cultivation of *T. vaginalis* with neutrophils. The enrichment of glycolytic enzymes, including malic enzyme, GAPDH, MDH, and enolase, in the co-cultivation group suggests two potential roles: enhancing metabolic efficiency and engaging in their

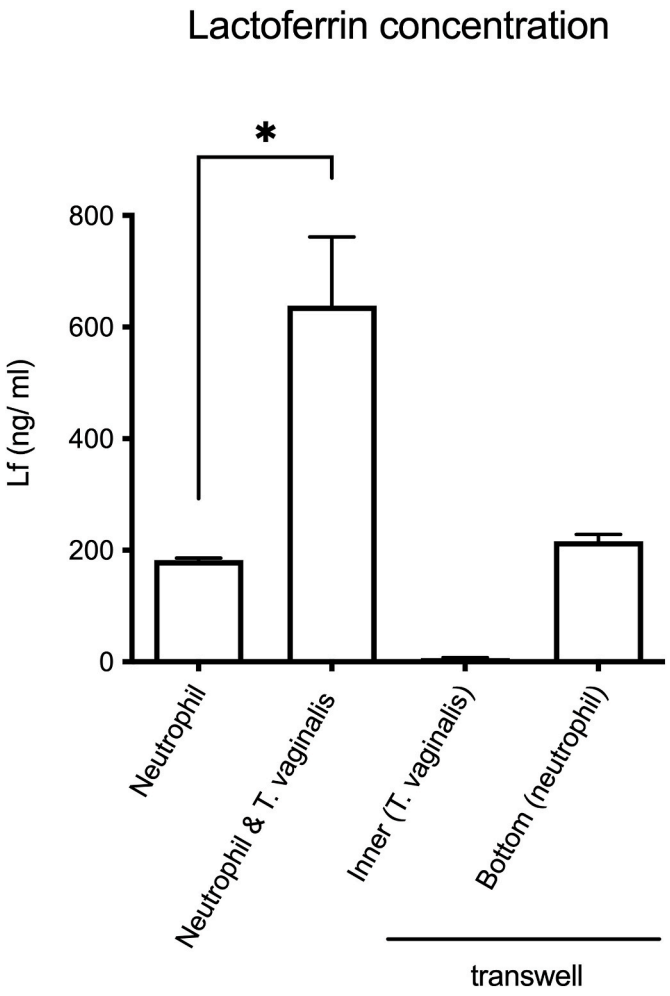

Fig. 4. Lactoferrin secretion is a contact-dependent process in neutrophils after *T. vaginalis* stimulation. The level of lactoferrin secretion was monitored by ELISA. The co-culture was performed (1 h), and the lactoferrin (neutrophil & *T. vaginalis*) was measured compared to the neutrophil control. In the transwell assay, the trichomonad cells were seeded in the inner well, whereas the neutrophils were seeded in the bottom well. The levels of lactoferrin in the inner and bottom wells were assessed.

moonlighting functions, such as cytoadherence. The malic enzyme, known as AP65, is known to contribute to cytoadherence during colonization and exhibits increased abundance after co-cultivation with neutrophils. Similarly, the presence of GAPDH on the cell membrane of *T. vaginalis* is considered crucial for fibronectin interaction.[47] Consequently, GAPDH, MDH, and enolase, akin to that of AP65, are speculative and might indicate their involvement in moonlighting functions.

Apo-lactoferrin is a microbiocidal molecule that strategically sequesters free iron from the infection site to limit its availability to invading microorganisms.[25,30] A receptor-mediated endocytosis recycles the iron-saturated lactoferrin in mammalian cells.[48] Interestingly, *T. vaginalis* has evolved specific receptors, enabling it to compete with the holo-lactoferrin as a source of iron for its proliferation and metabolism.[21] Interestingly, the apo-lactoferrin has no such beneficial effect on *T. vaginalis*, further emphasizing the iron-carriage role of holo-lactoferrin.[49] While lactoferrin is mainly secreted from the exocrine glands and secondary granules of neutrophils, the origin of lactoferrin in the infected vagina remains unclear.[23] The fluctuating lactoferrin in the vagina is mainly supplemented by menstrual blood, implying that lactoferrin is low during pre-menstrual period.[27] Our study provides direct evidence of lactoferrin secretion from trichomonad-stimulated neutrophils, revealing a contact-dependent process. In addition, the secretion

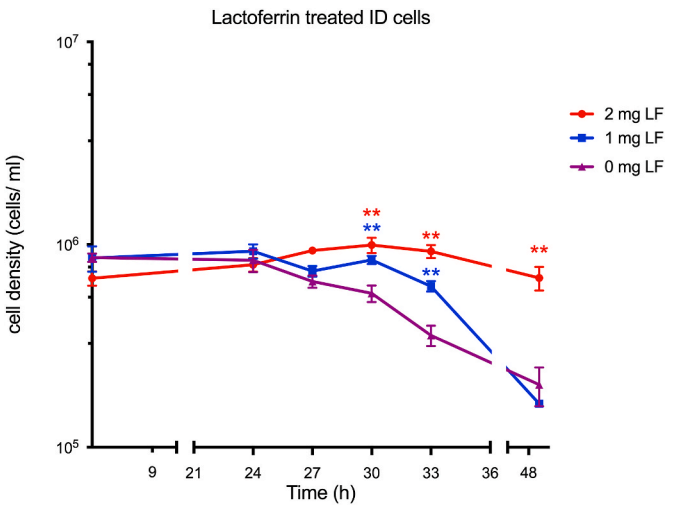

Fig. 5. Holo-lactoferrin extended the survival time of iron-deficient cultured *T. vaginalis*. The iron-loaded lactoferrin (LF, 1 and 2 mg/mL) was introduced into the iron-deficient culture system (180 μM dipyridyl), and the viability of trichomonad cells was monitored by trypan blue exclusion assay. The student-t tests were conducted to compare the control group to that of LF-treated groups (1 and 2 mg/mL). Significance is indicated by asterisks: $*P < 0.05$; $**P < 0.01$; $***P < 0.001$.

of LTB4-like molecule by *T. vaginalis* would attract the remote neutrophils to the infection site, and this might increase the opportunity of host-parasite interaction.[9] Our findings underscore the strategic attraction of neutrophils by *T. vaginalis* to the infection site to obtain iron from released lactoferrin.

5. Conclusion

In this work, our focus was on the interaction between *T. vaginalis* and neutrophils. We collected ESPs before and after co-cultivation, visualizing them through 2D gel electrophoresis. Most ESPs derived from neutrophils remained consistent before and after the protozoan stimulation, except lactoferrin. Neutrophils secreted lactoferrin contact-dependently after interaction with *T. vaginalis,* enhancing the parasite's survival under iron stress. Our findings emphasize the renewed role of neutrophils in *T. vaginalis* infection, particularly in providing apo-lactoferrin, which would be further loaded with iron and used by the protozoan. This discovery holds potential implications for the diagnosis and therapy of trichomoniasis.

CRediT authorship contribution statement

Wei-Hung Cheng: Writing – review & editing, Writing – original draft, Supervision, Funding acquisition, Conceptualization. **Ruei-Min Chen:** Methodology, Investigation, Formal analysis, Data curation. **Seow-Chin Ong:** Methodology, Investigation, Formal analysis, Data curation. **Yuan-Ming Yeh:** Visualization, Software, Methodology, Formal analysis, Data curation. **Po-Jung Huang:** Visualization, Software, Methodology, Investigation, Formal analysis, Data curation. **Chi-Ching Lee:** Visualization, Software, Methodology, Investigation, Formal analysis, Data curation.

Availability of data and materials

All data generated or analyzed during this study are included in this published article and its supplementary information files.

Declaration of generative AI in scientific writing

We state that any help from generative AI or AI assisted technology has not been obtained in writing of this manuscript.

Sources of funding

This work was supported by the National Science and Technology Council, Taiwan (NSTC 112-2320-B-006-054 and NSTC 113-2320-B-006-033) to WHC.

Declaration of competing interest

The authors declare that they have no competing interests.

Acknowledgments

We thank Prof. His-Hsien Lin and Ms. Chia-Jung Wu for their help in the neutrophil isolation.

Appendix A. Supplementary data

Supplementary data to this article can be found online at https://doi.org/10.1016/j.jmii.2024.11.004.

References

1. Johnston VJ, Mabey DC. Global epidemiology and control of *Trichomonas vaginalis*. *Curr Opin Infect Dis*. 2008;21:56–64.
2. Schwebke JR, Burgess D. Trichomoniasis. *Clin Microbiol Rev*. 2004;17:794–803.
3. Rowley J, Hoorn SV, Korenromp E, et al. Chlamydia, gonorrhoea, trichomoniasis and syphilis: global prevalence and incidence estimates, 2016. *Bull World Heal Organ*. 2019;97:548–562P.
4. Heine I, McGREGOR JA. *Trichomonas vaginalis*: a reemerging pathogen. *Clin Obstet Gynecol*. 1993;36:137.
5. Edwards T, Burke P, Smalley H, Hobbs G. *Trichomonas vaginalis*: clinical relevance, pathogenicity and diagnosis. *Crit Rev Microbiol*. 2016;42:406–417.
6. Kucknoor AS, Mundodi V, Alderete JF. The proteins secreted by *Trichomonas vaginalis* and vaginal epithelial cell response to secreted and episomally expressed AP65. *Cell Microbiol*. 2007;9:2586–2597.
7. Ryu J-S, Kang J-H, Jung S-Y, et al. Production of interleukin-8 by human neutrophils stimulated with *Trichomonas vaginalis*. *Infect Immun*. 2004;72:1326–1332.
8. Jarrett OD, Brady KE, Modur SP, et al. *T. vaginalis* infection is associated with increased IL-8 and TNFr1 levels but with the absence of CD38 and HLADR activation in the cervix of ESN. *PLoS One*. 2015;10, e0130146.
9. Shaio MF, Lin PR, Lee CS, Hou SC, Tang P, Yang KD. A novel neutrophil-activating factor released by *Trichomonas vaginalis*. *Infect Immun*. 1992;60:4475–4482.
10. Bhakta SB, Moran JA, Mercer F. Neutrophil interactions with the sexually transmitted parasite *Trichomonas vaginalis*: implications for immunity and pathogenesis. *Open Biol*. 2020;10, 200192.
11. Galego GB, Tasca T. Infinity war: *Trichomonas vaginalis* and interactions with host immune response. *Microb Cell*. 2023;10:103.
12. Frasson AP, Carli GAD, Bonan CD, Tasca T. Involvement of purinergic signaling on nitric oxide production by neutrophils stimulated with *Trichomonas vaginalis*. *Purinergic Signal*. 2012;8:1–9.
13. Mercer F, Ng SH, Brown TM, Boatman G, Johnson PJ. Neutrophils kill the parasite *Trichomonas vaginalis* using trogocytosis. *PLoS Biol*. 2018;16, e2003885.
14. Mercer F, Diala FGI, Chen Y-P, Molgora BM, Ng SH, Johnson PJ. Leukocyte lysis and cytokine induction by the human sexually transmitted parasite *Trichomonas vaginalis*. *PLoS Neglected Trop Dis*. 2016;10, e0004913.
15. Han IH, Park SJ, Ahn MH, Ryu JS. Involvement of mast cells in inflammation induced by *Trichomonas vaginalis* via crosstalk with vaginal epithelial cells. *Parasite Immunol*. 2012;34:8–14.
16. Song M-J, Lee J-J, Nam YH, et al. Modulation of dendritic cell function by *Trichomonas vaginalis*-derived secretory products. *BMB Rep*. 2015;48:103–108.
17. Twu O, Miguel N de, Lustig G, et al. *Trichomonas vaginalis* exosomes deliver cargo to host cells and mediate host:parasite interactions. *PLoS Pathog*. 2013;9, e1003482.
18. Twu O, Dessí D, Vu A, et al. *Trichomonas vaginalis* homolog of macrophage migration inhibitory factor induces prostate cell growth, invasiveness, and inflammatory responses. *Proc Natl Acad Sci*. 2014;111:8179–8184.
19. Nam YH, Min A, Kim SH, et al. Leukotriene B(4) receptors BLT1 and BLT2 are involved in interleukin-8 production in human neutrophils induced by *Trichomonas vaginalis*-derived secretory products. *Inflamm Res : Off J Eur Histamine Res Soc al*. 2011;61:97–102.
20. Min A, Lee YA, Kim KA, El-Benna J, Shin MH. SNAP23-dependent surface translocation of leukotriene B4 (LTB4) receptor 1 is essential for NOX2-mediated exocytotic degranulation in human mast cells induced by *Trichomonas vaginalis*-secreted LTB4. *Infect Immun*. 2016;85.
21. Lehker MW, Alderete JF. Iron regulates growth of *Trichomonas vaginalis* and the expression of immunogenic trichomonad proteins. *Mol Microbiol*. 1992;6:123–132.
22. Cheng W-H, Huang K-Y, Huang P-J, et al. Nitric oxide maintains cell survival of *Trichomonas vaginalis* upon iron depletion. *Parasites Vectors*. 2015;8:393.
23. Broxmeyer HE, Smithyman A, Eger RR, Meyers PA, Sousa M de. Identification of lactoferrin as the granulocyte-derived inhibitor of colony-stimulating activity production. *J Exp Med*. 1978;148:1052–1067.
24. Liang L, Wang Z-J, Ye G, et al. Distribution of lactoferrin is related with dynamics of neutrophils in bacterial infected mice intestine. *Molecules*. 2020;25:1496.
25. Weinberg ED. Iron availability and infection. *Biochim Biophys Acta Gen Subj*. 2009;1790:600–605.
26. Valenti P, Rosa L, Capobianco D, et al. Role of *Lactobacilli* and lactoferrin in the mucosal cervicovaginal defense. *Front Immunol*. 2018;9:376.
27. Ortz-Estrada G, Luna-Castro S, Pia-Vzquez C, et al. Iron-saturated lactoferrin and pathogenic protozoa: could this protein be an iron source for their parasitic style of life? *Future Microbiol*. 2012;7:149–164.
28. Mikulic N, Uyoga MA, Mwasi E, et al. Iron absorption is greater from apo-lactoferrin and is similar between holo-lactoferrin and ferrous sulfate: stable iron isotope studies in Kenyan infants. *J Nutr*. 2020;150:3200–3207.
29. Lambert LA. Molecular evolution of the transferrin family and associated receptors. *Biochim Biophys Acta Gen Subj*. 2012;1820:244–255.
30. Reyes-López M, Ramírez-Rico G, Serrano-Luna J, Garza M. de la. Activity of apo-lactoferrin on pathogenic protozoa. *Pharmaceutics*. 2022;14:1702.
31. Diamond LS, Clark CG, Cunnick CC. YI-S, a casein-free medium for axenic cultivation of *Entamoeba histolytica*, Related *Entamoeba, Giardia intestinalis* and *Trichomonas vaginalis*. *J Eukaryot Microbiol*. 1995;42:277–278.
32. Cheng W-H, Huang K-Y, Huang P-J, et al. γ-Carboxymuconolactone decarboxylase: a novel cell cycle-related basal body protein in the early branching eukaryote *Trichomonas vaginalis*. *Parasites Vectors*. 2017;10:443.
33. Huang K-Y, Chien K-Y, Lin Y-C, et al. A proteome reference map of *Trichomonas vaginalis*. *Parasitol Res*. 2008;104:927.
34. Shaio MF, Lin PR, Liu JY, Yang KD. Generation of interleukin-8 from human monocytes in response to *Trichomonas vaginalis* stimulation. *Infect Immun*. 1995;63:3864–3870.
35. Alderete JF, Nguyen J, Mundodi V, Lehker MW. Heme-iron increases levels of AP65-mediated adherence by *Trichomonas vaginalis*. *Microb Pathog*. 2004;36:263–271.
36. Peterson KM, Alderete JF. Iron uptake and increased intracellular enzyme activity follow host lactoferrin binding by *Trichomonas vaginalis* receptors. *J Exp Medicine*. 1984;160:398–410.
37. Arroyo R, Cárdenas-Guerra RE, Figueroa-Angulo EE, Puente-Rivera J, Zamudio-Prieto O, Ortega-López J. *Trichomonas vaginalis* cysteine proteinases: iron response in gene expression and proteolytic activity. *BioMed Res Int*. 2015;2015, 946787.
38. Olmos-Ortiz LM, Barajas-Mendiola MA, Barrios-Rodiles M, et al. *Trichomonas vaginalis* exosome-like vesicles modify the cytokine profile and reduce inflammation in parasite-infected mice. *Parasite Immunol*. 2017;39.
39. Cárdenas-Guerra RE, Arroyo R, Andrade IR de, Benchimol M, Ortega-López J. The iron-induced cysteine proteinase TvCP4 plays a key role in *Trichomonas vaginalis* haemolysis. *Microb Infect*. 2013;15:958–968.
40. Alvarez-Sánchez ME, Solano-González E, Yañez-Gómez C, Arroyo R. Negative iron regulation of the CP65 cysteine proteinase cytotoxicity in *Trichomonas vaginalis*. *Microb Infect*. 2007;9:1597–1605.
41. Provenzano D, Alderete JF. Analysis of human immunoglobulin-degrading cysteine proteinases of *Trichomonas vaginalis*. *Infect Immun*. 1995;63:3388–3395.
42. Alderete JF, Provenzano D, Lehker MW. Iron mediates *Trichomonas vaginalis* resistance to complement lysis. *Microb Pathog*. 1995;19:93–103.
43. Sulaiman AA, Zolnierczyk K, Japa O, et al. A trematode parasite derived growth factor binds and exerts influences on host immune functions via host cytokine receptor complexes. *PLoS Pathog*. 2016;12, e1005991.
44. Leontovyč A, Ulrychová L, O'Donoghue AJ, et al. SmSP2: a serine protease secreted by the blood fluke pathogen *Schistosoma mansoni* with anti-hemostatic properties. *PLoS Neglected Trop Dis*. 2018;12, e0006446.
45. Amiri P, Locksley RM, Parslow TG, et al. Tumour necrosis factor α restores granulomas and induces parasite egg-laying in schistosome-infected SCID mice. *Nature*. 1992;356:604–607.
46. Babayan SA, Read AF, Lawrence RA, Bain O, Allen JE. Filarial parasites develop faster and reproduce earlier in response to host immune effectors that determine filarial life expectancy. *PLoS Biol*. 2010;8, e1000525.
47. Lama A, Kucknoor A, Mundodi V, Alderete JF. Glyceraldehyde-3-phosphate dehydrogenase is a surface-associated, fibronectin-binding protein of *Trichomonas vaginalis*. *Infect Immun*. 2009;77:2703–2711.
48. Jiang R, Lopez V, Kelleher SL, Lönnerdal B. Apo- and holo-lactoferrin are both internalized by lactoferrin receptor via clathrin-mediated endocytosis but differentially affect ERK-signaling and cell proliferation in caco-2 cells. *J Cell Physiol*. 2011;226:3022–3031.
49. Lehker MW, Alderete JF. Iron regulates growth of *Trichomonas vaginalis* and the expression of immunogenic trichomonad proteins. *Mol Microbiol*. 1992;6:123–132.